WILEY-VCH

DOI: 10.1002/((please add manuscript number))
Article type: Communication

An apoferritin based drug delivery system for the tyrosine kinase inhibitor Gefitinib

*Anchala I. Kuruppu[a], Lei Zhang[b], Hilary Collins[a], Lyudmila Turyanska[c], Neil R. Thomas[b] and Tracey D. Bradshaw[a]**

[a)] A. I. Kuruppu, Dr H. Collins and Dr T. D. Bradshaw
Centre for Biomolecular Sciences, School of Pharmacy,
The University of Nottingham, Nottingham NG7 2RD, UK
* Tracey.Bradshaw@nottingham.ac.uk

[b)] L. Zhang and Prof N. R. Thomas
Centre for Biomolecular Sciences, School of Chemistry,
The University of Nottingham, Nottingham NG7 2RD, UK

[c)] Dr L. Turyanska
School of Physics and Astronomy,
The University of Nottingham, Nottingham NG7 2RD, UK

Keywords: apoferritin, Gefitinib, nanoparticles, breast cancer, drug delivery system

Development of a tumour-specific drug delivery system is challenging and depends immensely on the carrier. Currently various approaches are considered to develop efficient drug delivery systems.[1,2] Leaky vasculature, associated with sustained tumour angiogenesis together with tumour-associated poor lymphatic drainage can enhance passive targeting of nano-particles (NPs) to malignant tissue resulting in the enhanced permeability retention effect.[3,4] Nanoparticulate drug formulations, exploiting this feature of the tumour microenvironment, can be used to deliver chemotherapeutic agents to tumour target sites thereby increasing the therapeutic effect while minimising systemic toxicities.[5] When selecting a delivery system a major consideration is controlled release of the drug to the target site at a therapeutically optimal rate.[1,6]

Human ferritin is an ideal drug delivery carrier due to the nanoscale structure, and biocompatible, biodegradable, stable, non-toxic properties.[2,7,8] Ferritin consists of an apoferritin (AFt) protein cage and an iron core, and prevents accumulation of toxic levels of free iron in cells. AFt is composed of 24 subunits arranged into a 12 nm diameter cage with an internal 8 nm cavity. AFt is comprised of heavy (H) and light (L) chains which are highly homologous but functionally distinct. The AFt cage has 14 channels, each 3-4 Å in diameter, to allow exchange of cargo between the protein cage interior and exterior environments. Among the 14 channels, 8 are hydrophilic and 6 are hydrophobic.[6,7,9] Also, the AFt cage can disassemble into subunits at low pH (< pH 4.0) allowing release of cargo, and reassemble at higher pH (> pH 5.0).[5] Ferritin circulates and binds to a variety of cell types, however, specific binding to cells has been seen only for H-ferritins.[10] Ferritin binding sites and endocytosis of ferritin have been found in neoplastic cells,[11] and were associated with membrane specific transferrin receptors (TfR) that are highly expressed in many cancers[12] including breast and brain cancer cells.[12,13] The unique architecture of AFt provides two interfaces: the outer surface of AFt can be modified chemically or genetically with functional motifs[14]

and the internal cavity can be used to encapsulate pharmaceutical agents such as anti-cancer drugs, MRI and fluorescent imaging agents.[6,9,15,16] Recently, selective targeting and cargo delivery with H-AFt was demonstrated both *in vitro*[17] and *in vivo*.[18]

Gefitinib ('Iressa', ZD1839) is an orally active, epidermal growth factor receptor (EGFR) tyrosine kinase inhibitor.[19] This receptor family comprises four homologous receptors: EGFR (ErbB1/HER1), HER2 (ErbB2), HER3 (ErbB3) and HER4 (ErbB4), which have an extracellular ligand binding domain, a single hydrophobic trans-membrane domain and a cytoplasmic tyrosine kinase domain. These receptors are activated by either homo- or hetero-dimerisation upon ligand binding resulting in phosphorylation of specific tyrosine residues.[20,21] The overexpression of EGFR and HER2 in breast cancer, is associated with poor prognoses.[20,22,23] Gefitinib is used for treatment of EGFR and HER2 overexpressing breast cancers.[24,25] However, the therapeutic window of this drug is drastically narrowed by poor bioavailability, acquired resistance due to insufficient or ineffective cellular uptake and systemic toxicity resulting from interactions between drug and healthy tissue.[19,26] Also, orally administered Gefitinib is taken up extensively by human serum albumin and hence other delivery systems such as liposomes have been investigated.[27] Development of a selective targeted delivery system would improve efficiency of Gefitinib treatment.

Herein we report the use of human heavy chain apoferritin (H-AFt) as a delivery cage for Gefitinib to improve drug selectivity for HER2 overexpressing cells. The H-AFt-encapsulated-Gefitinib (H-AFt/Gefitinib) nanocomposite has potent and enhanced anti-tumour activity against the HER2 overexpressing SKBR3 breast cancer cell line (GI_{50} = 0.52 μM) compared to Gefitinib alone (GI_{50} = 1.66 μM; Table 1). Enhanced drug efficacy is achieved through sustained controlled drug release from the H-AFt cavity. In contrast, H-AFt-encapsulated-Gefitinib treatment of MDA-MB-231 breast cancer cell line, which does not express HER2, has shown decreased uptake of

Gefitinib compared to treatment with un-encapsulated drug. These results expose prospects for utilisation of H-AFt as a carrier for targeted delivery of anti-cancer drugs to HER2 over-expressing tumours.

For efficient entrapment of any drug into a delivery system, consideration of physical properties of both the drug and delivery system is important. Gefitinib is a hydrophobic drug and H-AFt has 6 hydrophobic channels allowing the drug molecules to enter the H-AFt cavity by passive diffusion during mixing of the drug with the protein (**Figure 1a**).[28] Gefitinib has low solubility in aqueous buffers[29] and was first dissolved in DMSO and then diluted with PBS at pH 7.2. This 1 mM aqueous solution of Gefitinib was mixed with H-AFt. The lateral dimensions of Gefitinib are < 0.3 nm, allowing Gefitinib intake through 6 hydrophobic channels by diffusion. The resulting solution was exhaustively dialysed and centrifuged at high speed to remove any un-encapsulated Gefitinib and any impurities. The encapsulation of Gefitinib was confirmed by UV spectrophotoscopy. Absorbance of Gefitinib was analysed at 250 nm and the encapsulation efficiency (EE) was quantified according to the Beer-Lambert law to be ~ 55%.

Mass spectrometry measures the mass to charge ratio and can be used to determine the purity and the molar mass of the particles.[30] Matrix-enriched laser desorption ionisation (MALDI) studies revealed high intensity peaks for H-AFt and Gefitinib which indicates high abundance of the drug and the protein in the mixture corresponding to a H-AFt molecular weight (MW) of 24.71 kDa and Gefitinib MW of 442.6 Da, comparable to the expected values (Supporting Information, S1). Protein determination by Bradford assay revealed 1.25 mg H-AFt/ml – equivalent to 50.6 µM. UV spectrophotometry determined a ratio of 605 µM Gefitinib / 50.6 µM H-AFt indicating > 10 molecules of Gefitinib per H-AFt cavity. Further evidence of Gefitinib

encapsulation within H-AFt was provided by flow cytometry analysis (Supporting Information, S1).

The stability and the structural integrity of H-AFt-encapsulated-Gefitinib were confirmed by PAGE and TEM. PAGE profile of H-AFt-encapsulated-Gefitinib revealed a band similar to that of H-AFt only, at MW ~ 24.7 kDa (**Figure 1b**). This indicates that the AFt protein structure and charge remain unchanged after encapsulation of Gefitinib. TEM images (**Figure 1c**) show intact H-AFt shells with an outer diameter of 13 ± 1 nm, and confirm that the H-AFt-encapsulated-Gefitinib retains the spherical shape and the size expected for H-AFt. The electron density of Gefitinib molecules is similar to that of H-AFt, hence there was insufficient contrast to resolve encapsulated Gefitinib in TEM.

In vitro effects of H-AFt-encapsulated-Gefitinib were assessed using the HER2 over-expressing SKBR3 cell line that expresses low levels of EGFR. As a negative control MDA-MB-231 cell line was used which does not express HER2 but expresses high levels of EGFR.[24]

Cellular internalisation of H-AFt-encapsulated-Gefitinib was observed by confocal microscopy and compared to that of Gefitinib. SKBR3 and MDA-MB-231 cells were treated with H-AFt-encapsulated-Gefitinib, Gefitinib and H-AFt (5 μM) for 24 h (**Figure 2** and Supporting Information, S2). The fluorescence of Gefitinib is environmentally sensitive: peak excitation and emission depends upon environment polarity and is intense in nonpolar solvents.[31] This property has allowed cellular uptake and distribution studies to be performed. Intracellular Gefitinib was evident from the bright fluorescence observed within the cytoplasm of SKBR3 cells treated with H-AFt-encapsulated-Gefitinib. Cytoplasmic Gefitinib fluorescence was punctuate consistent with localisation in acidic lysosomes and endosomes within these cells.[31] SKBR3 cells treated with H-AFt alone appeared to be identical to control cells and did not show

fluorescence. Also MDA-MB-231 cells treated with H-AFt-encapsulated-Gefitinib did not show bright fluorescence compared to MDA-MB-231 cells treated with Gefitinib indicating uptake suppression.

The cellular uptake of H-AFt-encapsulated-Gefitinib was quantified using flow cytometry. SKBR3 and MDA-MB-231 cells were treated with H-AFt-encapsulated-Gefitinib or Gefitinib (5 μM) for 24 h and compared to control. Mean fluorescence was used as a measure of Gefitinib uptake by the cells **(Figure 1d)**. Significant uptake by SKBR3 and MDA-MB-231 cells were measured for Gefitinib. Uptake of H-AFt-encapsulated-Gefitinib by SKBR3 cells was also significant; however uptake of H-AFt-encapsulated-Gefitinib by MDA-MB-231 cells was not significant compared to control. Thus, qualitative observations of confocal microscopy were corroborated by flow cytometry analyses, and demonstrate successful internalisation of H-AFt-encapsulated-Gefitinib by HER2 over-expressing SKBR3 cells.

In order to study *in vitro* anti-tumour activity of H-AFt-encapsulated-Gefitinib, cells were incubated with H-AFt-encapsulated-Gefitinib, Gefitinib and H-AFt for 72 h and growth inhibition was determined by MTT assay (Table 1; **Figure 3a-b** and Supporting Information, S3). Interestingly, the SKBR3 cell line was sensitive to both Gefitinib (GI_{50} = 0.94 ± 0.49 μM) and H-AFt-encapsulated-Gefitinib (GI_{50} = 1.44 ± 0.49 μM). However, the reduced potency of H-AFt-encapsulated-Gefitinib compared to Gefitinib alone implies that encapsulated Gefitinib may require time to be released from the H-AFt cavity as it is processed by endosome and lysosome systems with a local pH gradually reducing.[31] Conversely the MDA-MB-231 cell line demonstrated significantly reduced sensitivity to both Gefitinib (GI_{50} = 21.80 ± 0.52 μM) and H-AFt-encapsulated-Gefitinib (GI_{50} > 25 μM).

Although Gefitinib is an EGFR tyrosine kinase inhibitor, no correlation was observed between EGFR expression and sensitivity of cells. Gefitinib activity requires

a phosphorylated (active) form of EGFR whereas MDA-MB-231 cells express non-phosphorylated EGFR and hence are not sensitive to this drug.[24] On the other hand, cancer cells that express low levels of EGFR together with overexpression of HER2 are sensitive to this drug and indeed, high sensitivity of SKBR3 cells to Gefitinib was observed.[24,25] HER2 remains the preferred dimerisation partner of other ErbB receptors. Although both homo- and hetero-dimerisation activate the EGFR network, heterodimers are found to be more potently mitogenic and HER2 heterodimers generate the strongest biological activity compared to other heterodimers.[20,24,32]

TfR1 is associated with uptake of H-AFt and is more highly expressed in cancer cells compared to normal human cells.[12] It has been found that the expression of TfR1 correlates with tumour stage or cancer progression.[4] Iron is required by many cellular processes such as metabolism and DNA synthesis. TfR1 resides on cell membranes and imports cargo by receptor mediated endocytosis *via* clathrin-coated pits.[4,8] Both SKBR3 and MDA-MB-231 cells possess high levels of TfR1[33] which would assist cellular uptake of H-AFt-encapsulated-Gefitinib.[34] The greater SKBR3 growth inhibition by H-AFt compared to MDA-MB-231 implies greater sequestration of H-AFt by SKBR3 cells. Indeed, it has been shown previously that ferritin was not taken up by MDA-MB-231 cells.[35] In this study, the enhanced activity of H-AFt-encapsulated-Gefitinib in HER2 overexpressing cells is also a consequence of Gefitinib inhibition of kinase activity and therefor EGFR signalling triggered by HER2-EGFR dimerisation.

To determine whether a longer exposure time to encapsulated drug would be more effective in cells, MTT assays were performed following 120 h treatment (Table 1, **Figure 3c-d**). Again the SKBR3 cell line showed greater sensitivity to H-AFt alone compared to MDA-MB-231 cells. Interestingly the GI_{50} value for H-AFt-encapsulated-

Gefitinib (0.52 ± 0.17 μM) against the SKBR3 cell line was lower compared to the 72 h assay (GI_{50} = 1.44 ± 0.49 μM) and it was also lower (~ 3-fold) than that of Gefitinib after 120 h exposure (GI_{50} = 1.66 ± 0.79 μM). No significant difference was found between the GI_{50} values of Gefitinib alone at 72 and 120 h. It should be noted that at H-AFt-encapsulated-Gefitinib GI_{50} values of 1.44 μM and 0.52 μM, equivalent concentrations of AFt were 0.11 μM and 0.04 μM respectively, concentrations which negligibly impact SKBR3 cellular proliferation. Consistent with results following 72 h exposure, after 120 h exposure, the MDA-MB-231 cell line did not show sensitivity to H-AFt-encapsulated-Gefitinib, GI_{50} > 25 μM (equivalent to 2.1 μM AFt).

These results demonstrate that drug encapsulation enhances Gefitinib activity in SKBR3 cells and support the hypothesis that the H-AFt cage allows controlled release of drug molecules.

Tumour microenvironments exhibit lower extracellular pH than normal tissues while the intracellular pH of cells within normal and tumour cells is similar.[5] The overall pH range within a tumour environment is 6.5-7.2 where as normal cells possess a pH range of 7.2-7.4, allowing pH controlled release.[36] Further, the pH-dependent release of cargo could offer additional advantage for applications in stomach cancers, where an acidic environment would enhance drug release from the AFt cavity. Hence it was examined whether a more acidic *in vitro* environment would promote effective release of Gefitinib from its H-AFt cage. The investigations indicated that SKBR3 cells were unable to withstand pH < 7.0 environments for more than 72 h. However, at pH = 7.0, H-AFt-encapsulated-Gefitinib inhibited SKBR3 cell growth in a dose-dependent manner following 72 h exposure (GI_{50} = 0.44 ± 0.16 μM), exhibiting > 3-fold enhanced potency, compared to pH 7.5. Clonogenic assays were performed to determine whether individual SKBR3 cells were able to survive challenge with

Gefitinib or H-AFt-encapsulated-Gefitinib and subsequently form progeny colonies, indicative of tumour repopulation.[37] After 24 h exposure to agents followed by 13 days incubation with medium alone, H-AFt-encapsulated-Gefitinib demonstrated lower potency than Gefitinib **(Figure 4)**. The survival fraction (SF) of cells treated with Gefitinib was 50.7 ± 1.5% (1 μM) and 3.5 ± 1.0% (5 μM) compared to control whereas SF of cells treated with H-AFt-encapsulated-Gefitinib was 71.8 ± 0.5% (1 μM) and 34.4% ± 5.2% (5 μM). However, following 14 days continuous exposure to both agents, no colonies could be detected. These results endorse the premise of sustained drug release from H-AFt as an efficient drug delivery system.

Release of Gefitinib from H-AFt into buffer was examined at pH 2, 4 and 7.5 over a period of 24 h by analysing both the buffer and the solution retained within the dialysis bags. UV spectrometry was adopted to compare Gefitinib release from H-AFt. At pH 2 the AFt cage completely disassembles, at pH 4 the AFt cage swells, separating the protein sub-units and at pH 7.5 the AFt cage retains its assembled structure.[5] Rapid, cumulative diffusion of Gefitinib alone was observed at pH 7.5, reaching a plateau at 6 h. In comparison, at pH 2, 4 and 7.5, detection of Gefitinib released from H-AFt-encapsulated-Gefitinib indicates a slower cumulative release profile; progressively reduced drug was released from the AFt cage as pH increases (Supporting Information, S4). The most rapid cumulative release profile was observed at pH 2, consistent with the AFt cage disassembling and allowing Gefitinib release.

Analysis of residual buffer by flow cytometry (Supporting Information, S4) revealed only 2 negative populations at pH 2 and 4, exposing very low total fluorescence in the histograms relative to control. This implies that negligible amounts of Gefitinib were retained in the dialysis bags; after 24 h. However at pH 7.5, a small population positive for fluorescence was observed; indicating that some drug molecules remained

encapsulated, confirming sustained release of Gefitinib from H-AFt at physiological pH levels.[36]

The *in vitro* results indicate encapsulation of Gefitinib within an H-AFt cage could provide a facile route to targeted drug delivery and release *in vivo*. Recognition of H-AFt by TfR1 of cancer cells allows encapsulated cargo to be selectively internalised into cancer cells *via* TfR1 mediated endocytosis[3,4] and has successfully been utilised for targeted delivery of e.g. MRI imaging agents.[38] Although angiogenesis is enhanced in cancers[39] suggesting potential competition between endogenous ferritins and H-AFt uptake, a recent study demonstrated successful delivery of doxorubicin encapsulated in H-AFt to tumour sites and *in vivo* efficacy.[18] Thus we envisage that the observed selective targeting and enhanced efficacy could be translated *in vivo* and merits further detailed studies.

In conclusion successful encapsulation of Gefitinib within the H-AFt cavity, sustained release of cargo and subsequent anti-tumour activity selectively in HER2 overexpressing breast carcinoma cells is shown. Utilising the fluorescent property of Gefitinib it was able to confirm intracellular localisation of H-AFt-encapsulated-Gefitinib in SKBR3 cells. Potent, dose-dependent growth inhibition of cancer cells sensitive to EGFR inhibition was achieved and clonogenic assays further provided evidence of sustained Gefitinib release and significant *in vitro* anti-cancer activity of H-AFt-encapsulated-Gefitinib. H-AFt encapsulation could reduce off target toxicities of Gefitinib and diminish drug deposition in normal tissues. AFt encapsulation enhances the therapeutic efficacy of Gefitinib through passive targeted delivery and sustained release to tumour sites which demonstrates a successful nano-scale drug delivery system.

Experimental Section

Preparation and characterisation of H-AFt-encapsulated-Gefitinib: Gefitinib (Cayman Chemical USA) was dissolved in DMSO:PBS (1:1 at pH 7.2) at a concentration of 1 mM. 160 μM synthetic human H-AFt expressed in *E. coli* was provided by Prof. N. R. Thomas. There were additional His- and Avidin- tags and also linker sequences in the provided H-AFt. This increases the size of H-AFt from 21 kDa to ~ 24 kDa. H-AFt was added to Gefitinib solution with 40-fold excess of drug, and was stirred overnight at 4°C. The un-encapsulated Gefitinib was removed by dialysis in 20 mM Tris (pH 8.0) using a dialysis membrane (cut-off 8 kDa) for 48 h at 4°C. Any impurities were removed by centrifugation (13,000 rpm, 12 min, 4°C). The protein concentration of H-AFt was determined by Bradford assay.[40] The morphology was examined by transmission electron microscopy (TEM), (JEOL 2100F at 200 kV). For SDS-Polyacrylamide gel electrophoresis (PAGE), following denaturation (T = 95 °C for 5 min), 10 μl of H-AFt, H-AFt-encapsulated-Gefitinib and 5 μl of molecular marker (Thermo Scientific) were loaded onto a 4% stacking gel and resolved in a 12% resolving gel; samples were separated at 100 V for 2.5 h. The gel was stained overnight with 0.5% coomassie blue, followed by de-staining with 50% methanol and 10% acetic acid, and imaged in an UVP BioDoc-It system.

Determining encapsulation efficiency (EE): Absorbance of serial dilutions of Gefitinib (from 250 to 0.5 μM in DMSO) at 250 nm was analysed using Perkin Elmer Lambda 25 UV/VIS Spectrometer and WinLab ver 6.0.4.0738 and the Beer-Lambert law was used to quantify the encapsulated drug. The EE was estimated as a ratio between the concentration of the encapsulated drug and that used in synthesis.

Confirmation of encapsulation of Gefitinib in H-AFt: H-AFt-encapsulated-Gefitinib solution was analysed using an Astrios EQ flow cytometer (Beckman Coulter, Summit 6.2.3.1561) equipped with 488 nm and 355 nm lasers. Fluorescence emission was collected using a 405/30 band-pass filter.

Mass spectrometry: For matrix assisted laser desorption ionisation mass spectrometry (MALDI), H-AFt-encapsulated-Gefitinib (10 μl) was mixed with sinapic acid and 0.5 μl of the resulting solution was loaded onto a MALDI target sample plate. The plate was left to air dry for 5 min and was analysed on the Bruker Ultraflex III spectrometer.

Cell lines and cell culture: SKBR3 and MDA-MB-231 breast cancer cell lines (European Collection of Cell Cultures) were maintained in RPMI 1640 medium supplemented with 10% foetal bovine serum (FBS) at 37°C in a humidified atmosphere containing 5% CO_2.

MTT assay: Cells were seeded in 96 well plates (2.5 x 10^3 per well) 24 h before treatment with Gefitinib, H-AFt-encapsulated-Gefitinib and H-AFt. Following 72 h or 120 h exposure, MTT (3-(4,5-dimethylthiazol-2-yl)-2,5-diphenyltetrazolium bromide; 400 μg/ml) was added and plates were incubated for 2.5 h. Well supernatants were aspirated and formazan solubilised with 150 μl 100% DMSO. Absorbance at 550 nm was read on Perkin Elmer plate reader. 1 M HCl was introduced into medium drop-wise for MTT assays at pH 7.0.

Clonogenic assay: SKBR3 cells (250 per well) were seeded into 6 well plates and allowed 24 h to attach. Following 24 h treatment with Gefitinib and H-AFt-encapsulated-Gefitinib (1 μM and 5 μM), in half of the wells test agent was replaced with 2 ml of fresh medium. Cells in the remaining wells were exposed to test agents for 14 d. Experiments were terminated when colonies of ≥ 50 cells were formed in control wells. Colonies were washed (PBS), fixed (methanol; 15 min), stained (0.5% methylene blue; 15 min) and counted. Survival fractions (SF) were calculated: SF = Plating efficiency of treated sample / Plating efficiency of control x 100 %.[37]

Release of Gefitinib from H-AFt: Dialysis bags (cut-off 8 kDa) containing H-AFt-encapsulated-Gefitinib (100 μM) and Gefitinib (100 μM) diluted in 20 mM Tris buffer (900 μl) were placed in separate beakers containing 20 mM Tris buffer at pH 2, 4 or 7.5 at 37°C, 5% CO_2. Released Gefitinib was quantified after 2, 6, 12 and 24 h by UV spectrophotometry

at 250 nm. Gefitinib in the residual buffer within the dialysis bags was detected by Astrios EQ flow cytometry.

Cellular uptake studies: For confocal microscopy, SKBR3 and MDA-MB-231 (2 x 10^4) cells were seeded into 8 well coverslips and allowed to attach overnight. Following 24 h exposures with Gefitinib or H-AFt-encapsulated-Gefitinib (5 μM), live imaging of cells was carried out using a Zeiss LSM 510 fluorescence microscope equipped with a UV laser of 351 nm excitation and LP385 emission filter. For flow cytometry studies, SKBR3 and MDA-MB-231 cells (2.5 x 10^5) were seeded in 6 well plates and allowed to attach overnight before 24 h exposure to Gefitinib or H-AFt-encapsulated-Gefitinib (5 μM). Cells were washed and collected into FACS tubes. Using an Astrios EQ flow cytometer, 20,000 events were acquired and Gefitinib fluorescence was collected.

Statistical analyses: All experiments were repeated ≥3 times and results are presented as means ± SD (Standard Deviation) or ± SE (Standard Error). Significant differences were defined as $P < 0.05$.

Supporting Information

Supporting Information is available from the Wiley Online Library.

Acknowledgements

This work was supported by Schlumberger Faculty for the Future (FFTF) programme. Authors thank Dr. David Onion, Dr. Michael W. Fay and Melchior Cini for flow cytometry, transmission electron microscopy and UV spectrometry expertise respectively.

Received: ((will be filled in by the editorial staff))
Revised: ((will be filled in by the editorial staff))
Published online: ((will be filled in by the editorial staff))

References

1. Kumaresh S Soppimatha TMA, Anandrao R Kulkarnia and Walter E Rudzinskib. Biodegradable polymeric nanoparticles as drug delivery devices. *Journal of Controlled Release.* 2001;70:1-20.

2. Borm WHDJaPJA. Drug delivery and nanoparticles: Applications and hazards. *International Journal of Nanomedicine.* 2008;3:133-149.

3. Fabienne Danhier OFaVP. To exploit the tumor microenvironment: Passive and active tumor targeting of nanocarriers for anti-cancer drug delivery. *Journal of Controlled Release.* 2010;148:135-146.

4. Tracy R. Daniels EB, Jose A. Rodriguez, Shabnum Patel, Maggie Kozman, DiegoA. Chiappetta, Eggehard Holler, Julia Y. Ljubimova, Gustavo Helguera and Manuel L. Penichet. The transferrin receptor and the targeted delivery of therapeutic agents against cancer. *Biochimica et Biophysica Acta.* 2012;1820:291-317.

5. Aihui Ma-Ham HW, Jun Wang, Xinhuang Kang, Youyu Zhang and Yuehe Lin. Apoferritin-based nanomedicine platform for drug delivery: equilibrium binding study of daunomycin with DNA. *Journal of Materials Chemistry.* 2011;21:8700-8708.

6. Zhen Yang XW, Huajia Diao, Junfeng Zhang, Hongyan Li, Hongzhe Sun and Zijian Guo. Encapsulation of platinum anticancer drugs by apoferritin. *Chemical Communications.* 2007;33:3409-3500.

7. Aihui MaHam ZT, Hong Wu, Jun Wang and Yuehe Lin. Protein-Based Nanomedicine Platforms for Drug Delivery. *Small.* 2009;5:1706–1721.

8. Zbynek Heger SS, Ondrej Zitka, Vojtech Adam and Rene Kizek. Apoferritin applications in nanomedicine. *Nanomedicine.* 2014;9:2233-2245.

9. Lianbing Zhang LL, Wolfram Munchgesang, Eckhard Pippel, Ulrich Gosele, Matthias Brandsch and Mato Knez. Reducing Stress on Cells with Apoferritin-Encapsulated Platinum Nanoparticles. *Nano Letters.* 2010;10:219-223.

10. Li Li CJF, James C. Ryan, Erene C. Niemi, Jose A. Lebron, Pamela J. Bjorkman, Hisashi Arase, Frank M. Torti, Suzy V. Torti, Mary C. Nakamura and William E. Seaman. Binding and uptake of H-ferritin are mediated by human transferrin receptor-1. *Proceedings of the national academy of sciences of the United States of America.* 2010;107:3505-3510.

11. Lianbing Zhang WF, Eckhard Pippel, Gerd Hause, Matthias Brandsch and Mato Knez. Receptor-Mediated Cellular Uptake of Nanoparticles: A Switchable Delivery System. *Small.* 2011;7:1538-1541.

12. Torti SVTaFM. Iron and cancer:more ore to be mined. *Nature Reviews Cancer.* 2013;13:342-355.

13. Avi Schroeder DAH, Monte M. Winslow, James E. Dahlman, George W. Pratt, Robert Langer, Tyler Jacks and Daniel G. Anderson. Treating metastatic cancer with nanotechnology. *Nature Reviews Cancer.* 2012;12:39-50.

14. Zipeng Zhen, Wei Tang, Hongmin Chen, Xin Lin, Trever Todd, Geoffrey Wang, Taku Cowger, Xiaoyuan Chen and Jin Xie. RGD-Modified Apoferritin Nanoparticles for Efficient Drug Delivery to Tumors. *Acs Nano.* 2013;7:4830-4837.

15. Kilic MA, Ozlu E and Calis S. Novel Protein-Based Anticancer Drug Encapsulating Nanosphere: Apoferritin-Doxorubicin Complex. *J Biomed Nanotechnol.* 2012;8:508-514.

16. Simonetta Geninatti Crich, Benedetta Bussolati, Lorenzo Tei, Cristina Grange, Giovanna Esposito, Stefania Lanzardo, Giovanni Camussi and Silvio Aime. Magnetic resonance visualization of tumor angiogenesis by targeting neural cell adhesion

molecules with the highly sensitive gadolinium-loaded apoferritin probe. *Cancer Res.* 2006;66:9196-9201.

17. Fan K, Cao C, Pan Y, Lu D, Yang D, Feng J, Song L, Liang M and Yan X. Magnetoferritin nanoparticles for targeting and visualizing tumour tissues. *Nat Nanotechnol.* 2012;7:459-464.

18. Minmin Liang, Kelong Fan, Meng Zhou, Demin Duan, Jiyan Zheng, Dongling Yang, Jing Feng and Xiyun Yan. H-ferritin-nanocaged doxorubicin nanoparticles specifically target and kill tumors with a single-dose injection. *Proc. Natl. Acad. Sci. U.S.A.* 2014;111:14900-14905.

19. Martin H. Cohen GAW, Rajeshwari Sridhara, Gang Chen, W. David McGuinn, Jr., David Morse, Sophia Abraham, Atiqur Rahman, Chenyi Liang, Richard Lostritto, Amy Baird and Richard Pazdur. United States Food and Drug Administration Drug Approval Summary: Gefitinib (ZD1839; Iressa) Tablets. *Clinical Cancer Research.* 2004;10:1212-1218.

20. Mina D. Marmor KBSaYY. Signal transduction and oncogenesis by ErBb/HER receptors. *Int. J. Radiation Oncology Biol. Phys.* 2004;58:903–913.

21. Pines YYaG. The ERBB network: at last, cancer therapy meets systems biology. *Nature Reviews Cancer.* 2012;12:553-563.

22. Sara A. Hurvitz YH, Neil O'Brien and Richard S. Finn. Current approaches and future directions in the treatment of HER2-positive breast cancer. *Cancer Treatment Reviews.* 2013;39:219-229.

23. Subik K, Lee JF, Baxter L, et al. The Expression Patterns of ER, PR, HER2, CK5/6, EGFR, Ki-67 and AR by Immunohistochemical Analysis in Breast Cancer Cell Lines. *Breast Cancer (Auckl).* 2010;4:35-41.

24. Manuela Campiglio AL, Clelia Olgiati, Nicola Normanno, Giulia Somenzi, Lucia Vigano, Marzia Fumagalli, Sylvie Menard and Luca Gianni. Inhibition of Proliferation and Induction of Apoptosis in Breast Cancer Cells by the Epidermal Growth Factor Receptor (EGFR) Tyrosine Kinase Inhibitor ZD1839 ('Iressa') Is Independent of EGFR Expression Level. *Journal of Cellular Physiology.* 2004;198:259-268.

25. FR Hirsch MV-GaFC. Predictive value of EGFR and HER2 overexpression in advanced non-small-cell lung cancer. *Oncogene.* 2009;28:S32-S37.

26. A. Haringhuizen HvT, H. F. R. Vaessen, P. Baas and N. van Zandwijk. Gefitinib as a last treatment option for non-small-cell lung cancer: durable disease control in a subset of patients. *Annals of Oncology.* 2004;15:786-792.

27. Zhou X, Yung B, Huang Y, Li H, Hu X, Xiang G and Lee RJ. Novel Liposomal Gefitinib (L-GEF) Formulations. *Anticancer Res.* 2012;32:2919-2923.

28. Yijie Shi CS, Wenyu Cui, Hongdan Li, Liwei Liu, Bo Feng, Ming Liu, Rongjian Su and Liang Zhao. Gefitinib loaded folate decorated bovine serum albumin conjugated carboxymethyl-betacyclodextrin nanoparticles enhance drug delivery and attenuate autophagy in folate receptor-positive cancer cells *Journal of Nanobiotechnology.* 2014;12:43.

29. Amol Ashok Pawar D-RCaCV. Influence of precursor solvent properties on matrix crystallinity and drug release rates from nanoparticle aerosol lipid matrices. *International Journal of Pharmaceutics.* 2012;430:228-237.

30. Surya Prakash Gautam AKG, Shashank Agrawal and Shruti Sureka. Spectroscopic characterization of dendrimers. *International Journal of Pharmacy and Pharmaceutical Sciences.* 2012;4:77-80.

31. Brian J. Trummer VI, Sathy V. Balu-Iyer, Robert O'Connor and Robert M. Straubinger. Physicochemical properties of EGF receptor inhibitors and development of a nanoliposomal formulation of gefitinib. *Journal of pharmaceutical sciences.* 2012;101:2763-2776.

32. Dianne S. Hirsch, Yi Shen and Wen Jin Wu. Growth and motility inhibition of breast cancer cells by epidermal growth factor receptor degradation is correlated with inactivation of Cdc42. *Cancer Res.* 2006;66:3523-3530.

33. Megumi Kawamoto TH, Masayuki Kohno and Koji Kawakami. A novel transferrin receptor-targeted hybrid peptide disintegrates cancer cell membrane to induce rapid killing of cancer cells. *BMC Cancer.* 2011;11:2-13.

34. Yu Zheng BY, Wanlop Weecharangsan, Longzhu Piao, Michael Darby, Yicheng Mao, Rumiana Koynova, Xiaojuan Yang, Hong Li, Songlin Xu, L. James Lee, Yasuro Sugimoto, Robert W. Brueggemeier and Robert J. Lee. Transferrin-conjugated lipid-coated PLGA nanoparticles for targeted delivery of aromatase inhibitor 7 -APTADD to breast cancer cells. *International Journal of Pharmaceutics.* 2010;390:234-241.

35. Ahmed A. Alkhateeb BHaJRC. Ferritin stimulates breast cancer cells through an ironindependent mechanism and is localized within tumor-associated macrophages. *Breast Cancer Research and Treatment.* 2013;137:733-744.

36. Eun Seong Lee ZGaYHB. Recent progress in tumor pH targeting nanotechnology. *Journal of Controlled Release.* 2008;132:164-170.

37. Nicolaas A P Franken HMR, Jan Stap, Jaap Haveman and Chris van Bree. Clonogenic assay of cells in vitro. *Nature Protocols.* 2006;1:2315-2319.

38. Kelong Fan, Changqian Cao, Yongxin Pan, Di Lu, Dongling Yang, Jing Feng, Lina Song, Minmin Liang and Xiyun Yan. Magnetoferritin nanoparticles for targeting and visualizing tumour tissues. *Nat Nanotechnol.* 2012;7:459-464.

39. Lan G. Coffman, Derek Parsonage, Ralph D'Agostino, Frank M. Torti, and Suzy V. Torti. Regulatory effects of ferritin on angiogenesis. *Proc. Natl. Acad. Sci. U.S.A.* 2009;106:570-575.

40. Bradford MM. A rapid and sensitive method for the quantitation of microgram quantities of protein utilizing the principle of protein-dye binding. *Analytical Biochemistry.* 1976;72:248-254.

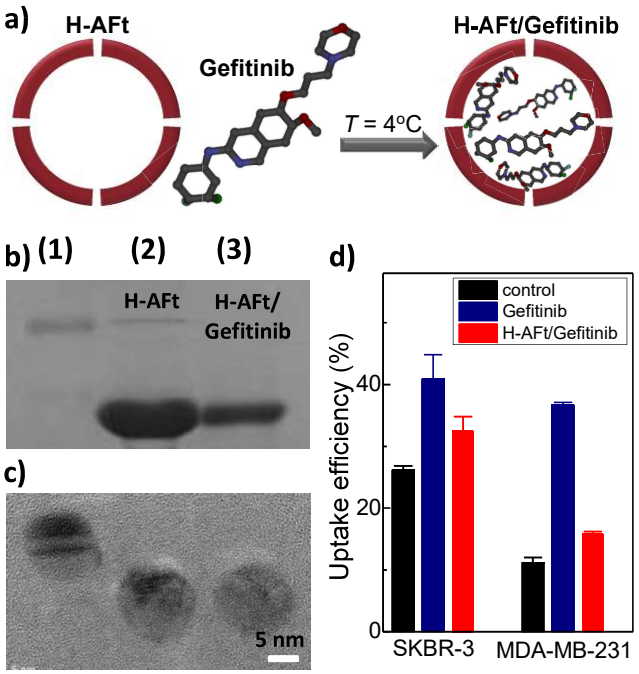

Figure 1. (a) Schematic representation of preparation of H-AFt-encapsulated-Gefitinib encapsulated NPs. **(b)** PAGE- (1) Marker (2) H-AFt (3) H-AFt-encapsulated-Gefitinib. **(c)** TEM Images of H-AFt/Gefitinib confirming the size of the NPs. **(d)** Mean fluorescence uptake by SKBR3 and MDA-MB-231 cells using flow cytometry. Mean and SD of 3 independent trials (n = 2 per trial).

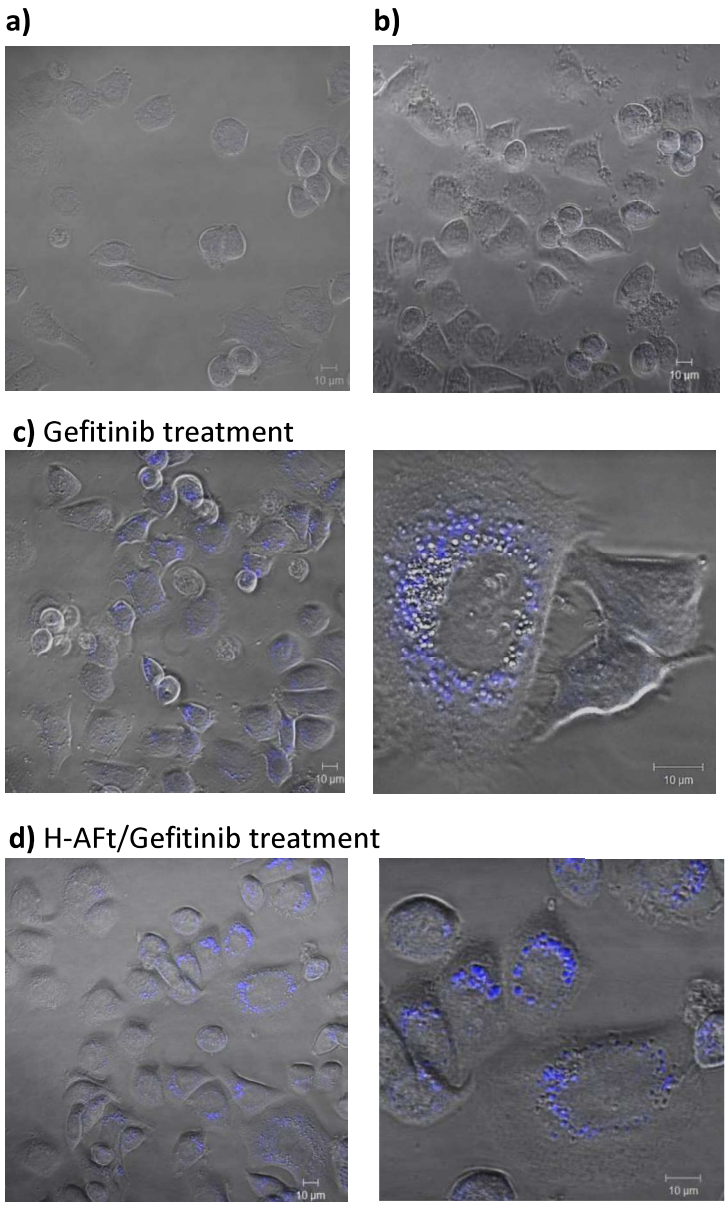

Figure 2. Confocal microscopy images of SKBR3 cells demonstrating cellular uptake of Gefitinib after 24 h exposure of cells to: **(a)** control, **(b)** H-AFt, **(c)** Gefitinib, **(d)** H-AFt-encapsulated-Gefitinib. Representative images of 3 independent trials are shown (n = 2 per trial).

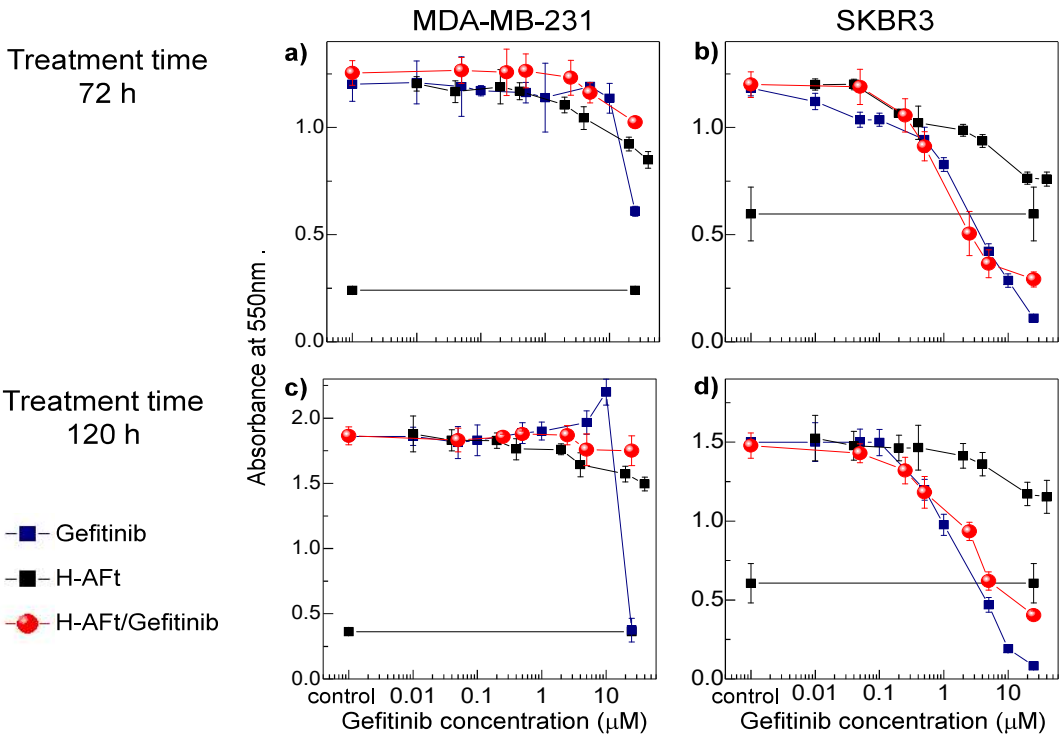

Figure 3. Representative growth inhibitory curves for Gefitinib, H-AFt and H-AFt-encapsulated-Gefitinib. MDA-MB-231 The concentration of for the H-AFt only sample is normalised to the concentration of AFt in H-AFt-encapsulated-Gefitinib. **(a, c)** and SKBR3 **(b, d)** cells were seeded at a density of 2.5 x 10^3 in 96 well plates at pH 7.5. Following 72 h **(a, b)** or 120 h **(c, d)** exposure to test agents, cell growth and viability were determined by MTT assays. Mean and SD of representative experiments of ≥ 3 independent trials are shown (n = 8 per trial).

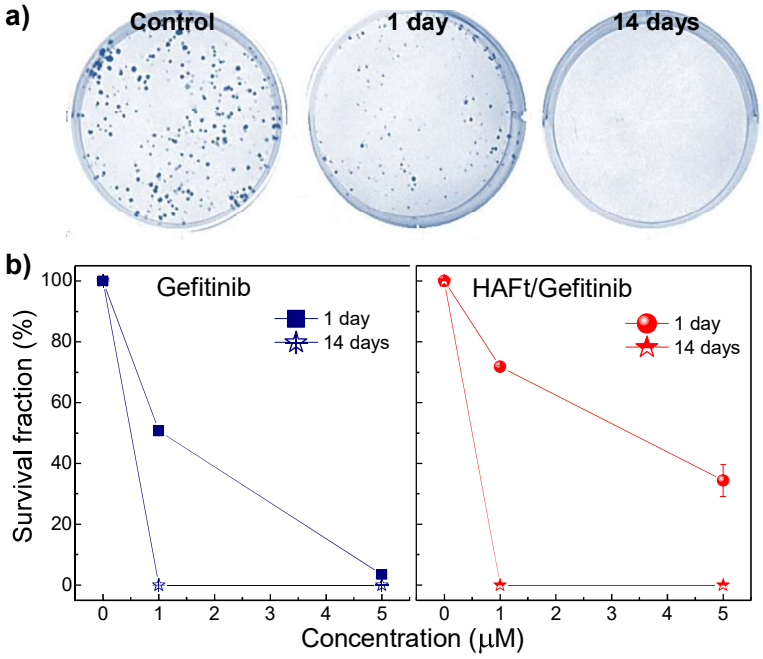

Figure 4. (a) Photographs of SKBR3 colonies following treatment of cells with 5 μM H-AFt-encapsulated-Gefitinib. **(b)** Effect of Gefitinib and H-AFt-encapsulated-Gefitinib treatment on SKBR3 colony formation. Cells were exposed to drug for 14 days continuously or for 24 h only (1 day) followed by 13 days in medium alone. Mean and SD of 3 independent trials (n = 3 per trial).

Table 1. Effect of Gefitinib, H-AFt-encapsulated-Gefitinib and H-AFt on growth of SKBR3 and MDA-MB-231 cells. It should be noted that the GI_{50} values for H-AFt-encapsulated-Gefitinib refer to encapsulated Gefitinib concentration; the amount of Gefitinib encapsulated per H-AFt cage impacts material potency and merits futher detailed studies.

	Mean GI_{50} value ± SE (μM)					
	Gefitinib		**H-AFt-encapsulated-Gefitinib**		**H-AFt**	
Cell line	**72 h**	**120 h**	**72 h**	**120 h**	**72 h**	**120 h**
SKBR3	0.94 ± 0.49	1.66 ± 0.79	1.44 ± 0.49	0.52 ± 0.17	4.84 ± 4.80	5.50 ± 3.81
MDA-MB-231	21.80 ± 0.52	19.56 ± 0.64	>25	>25	16.47 ± 0.98	19.85 ± 0.15

The table of content

Anti-cancer drug Gefitinib encapsulated within human heavy chain apoferritin by diffusion; allows pH –controlled sustained release of cargo. The combination of increased cellular uptake, and potent and enhanced anti-tumour activity against the HER2 over-expressing SKBR3 cell line compared to Gefitinib alone, makes it a promising carrier for delivery of drugs to tumour sites.

Keyword Apoferritin-Gefitinib

A. I. Kuruppu, L. Zhang, H. Collins, L. Turyanska, N. R. Thomas and T. D. Bradshaw

An apoferritin based drug delivery system for the tyrosine kinase inhibitor-Gefitinib

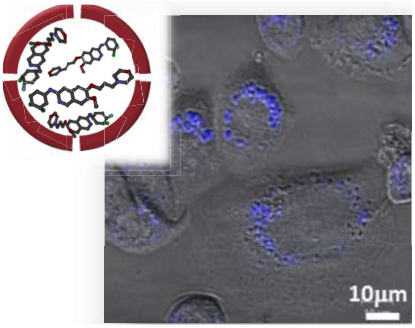

Supporting Information

An apoferritin based drug delivery system for the tyrosine kinase inhibitor-Gefitinib

*Anchala I. Kuruppu, Lei Zhang, Hilary Collins, Lyudmila Turyanska, Neil R. Thomas and Tracey D. Bradshaw**

S1 Probing encapsulation by flow cytometry and MALDI.

As Gefitinib is fluorescent under UV, H-AFt-encapsulated-Gefitinib was observed using excitation and emission wavelengths of 355 and 385 nm respectively by the 405/30 band pass filter of the Astrios EQ flow cytometer. Fluorescence was detected by the forward scatter (FSC) and a marker was placed to detect the populations positive (R3) and negative (R4) for fluorescence. Figure S1.1 a shows a histogram of H-AFt, in which Gefitinib was not encapsulated, thus showing only a negative population on to the left with very little fluorescence. However after encapsulation of Gefitinib within the H-AFt cavity, a large positive population denoted by a fluorescence shift to the right was detected with a fluorescence population 180-times brighter than H-AFt alone (Figure S1.1 b). These data confirm encapsulation of Gefitinib within AFt cage.

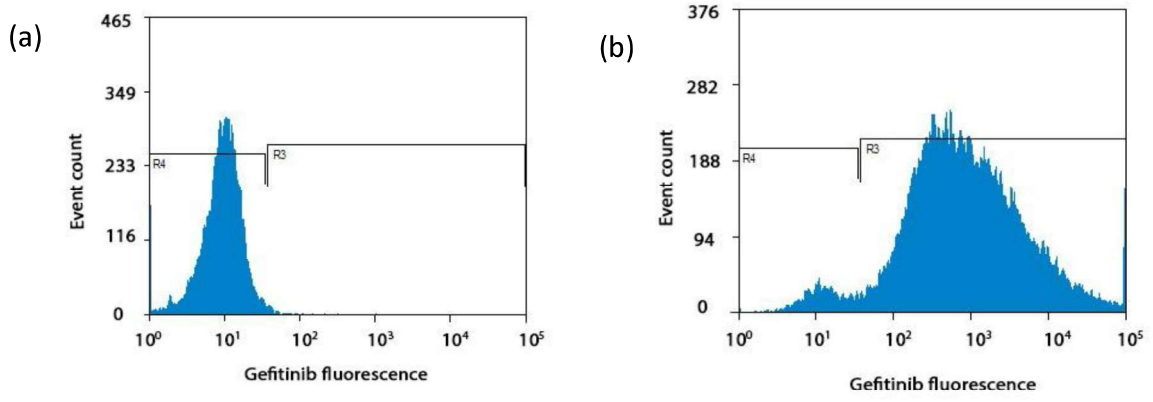

Figure S1.1. Flow cytometry histograms confirming the encapsulation of Gefitinib in H-AFt. **a)** H-AFt only and **b)** H-AFt-encapsulated-Gefitinib.

Matrix-enriched laser desorption ionisation (MALDI) studies revealed high intensity peaks (Figure S1.2) for H-AFt and Gefitinib which indicates high abundance of the drug and the protein in the mixture corresponding to a H-AFt molecular weight (MW) of 24.71 kDa and Gefitinib MW of 442.6 Da, comparable to the expected values.

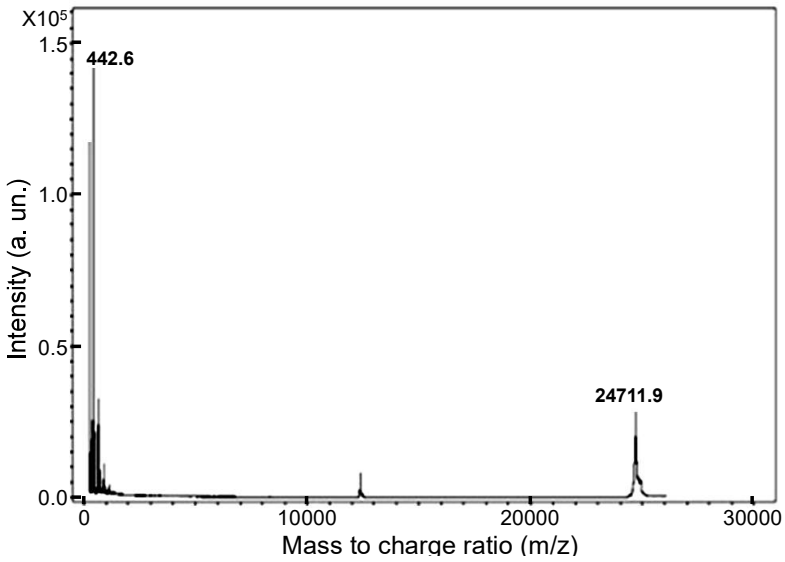

Figure S1.2. MALDI spectrum of H-Aft encapsupated Gefitinib

S2 Cellular uptake of MDA-MB-231 cells by confocal microscopy.

MDA-MB-231 cells (2 x 10^4) were seeded into 8 well chambered coverslips and allowed to attach overnight. Cells were then treated with 5 μM of Gefitinib or H-AFt-encapsulated-Gefitinib. After 24 h, live imaging of cells was carried out using a fluorescence confocal microscope. Cells treated with 5 μM H-AFt-encapsulated-Gefitinib (Figure S2 c) did not show bright fluorescence compared to those exposed to Gefitinib (Figure S2 b).

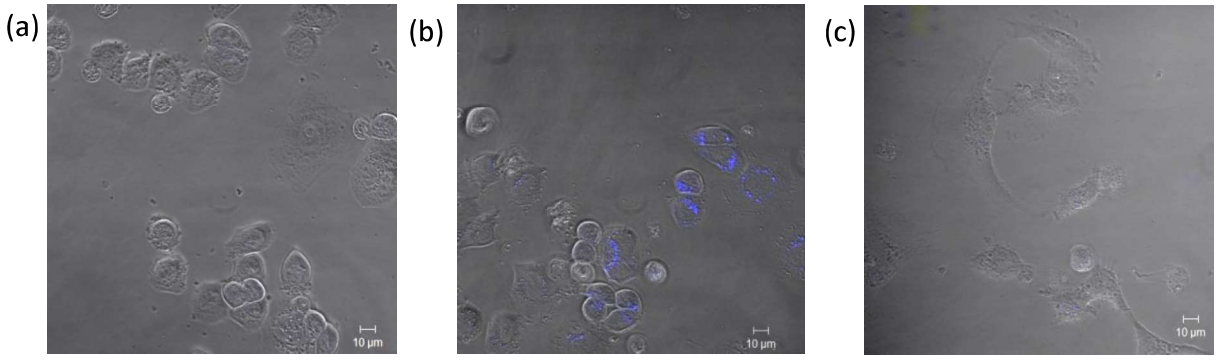

Figure S2. Confocal microscopy images of MDA-MB-231 cells demonstrating cellular uptake of Gefitinib after 24 h exposure of cells to: (a) control, (b) Gefitinib (c) H-AFt-encapsulated-Gefitinib. Representative images of 3 independent trials (n = 2 per trial).

S3 H-AFt-encapsulated-Gefitinib induced growth inhibition.

Tumour microenvironments exhibit lower extracellular pH than normal tissues while the intracellular pH of cells within normal and tumour cells is similar.[36] This acidic enviornment may help to relase the encapsulated cargo. Hence it was tested whether a more acidic *in vitro* environment would promote effective release of Gefitinib from H-AFt cage (Figure S3). Lower GI_{50} values were observed at pH 7.0 following 72 h exposure compared to normal pH (pH 7.5) conditions for H-AFt-encapsulated-Gefitinib (GI_{50} = 0.44 ± 0.16 µM). Gefitnib also showed low GI_{50} values at pH = 7.0 (GI_{50} = 0.13 ± 0.06 µM).

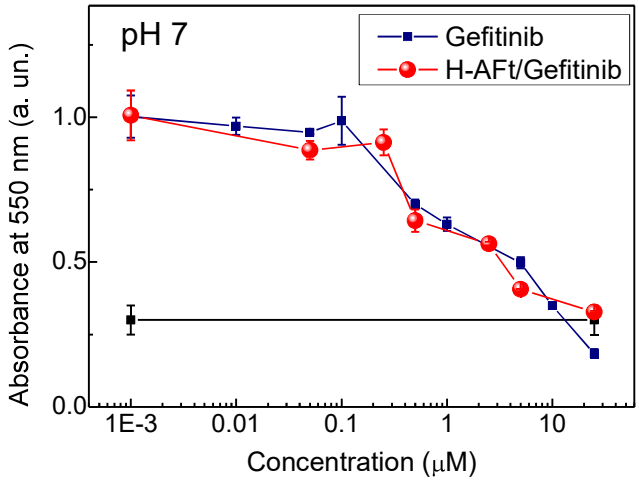

Figure S3. Representative growth inhibitory curves for H-AFt-encapsulated-Gefitinib and Gefitinib. SKBR3 cells were seeded at a density of 2.5 x 10^3 in 96 well plates at pH 7.0. Cells were treated after 24 h and exposed to agent for 72 h. Mean and SD of representative experiments of ≥ 3 independent trials are shown (n = 8 per trial).

S4 pH induced drug release.

H-AFt cage is pH sensitive thus allowing the control of drug release by the properties of the environment.[5] The pH dependent reassembly property of AFt could be advantageous for applications in tumours where extracellular pH is lower than in normal tissues and in stomach cancers, where an acidic environment would enhance the drug release from the AFt cavity. UV spectrometry was adopted to compare Gefitinib release from H-AFt at pH 2, 4 and 7.5. Release of Gefitinib alone was observed only at pH 7.5. By analysing the buffer which was released from the dialysis bags it was observed that Gefitinib showed a rapid release profile with a higher % of drug release. Gefitinib release reached a plateau phase at 6 h. In comparison at pH 2, 4 and 7.5, H-AFt-encapsulated-Gefitinib showed a slower cumulative release profile and a lower % of drug release due to being encapsulated in the AFt cavity. Among the pH levels the fastest cumulative release profile was observed for H-AFt-encapsulated-Gefitinib at pH 2 (Figure S4 a).

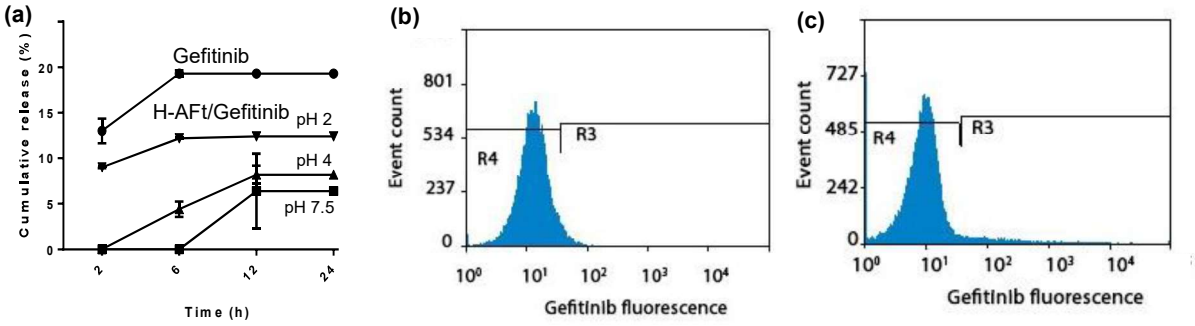

Figure S4. Detection of Gefitinib released from H-AFt cavity **(a)** Cumulative release of Gefitinib alone at pH 7.5 and from H-AFt-encapsulated-Gefitinib at pH 2, 4 and 7.5 at 2, 6, 12 and 24 h observed by UV spectrometry. **(b and c)** Representative histograms representing fluorescence emitted by Gefitinib. A marker was placed to detect the positive (R3) and the negative (R4) populations for fluorescence. (b) Residual H-AFt alone, (c) Residual H-AFt-encapsulated-Gefitinib (pH 7.5). Mean and SD of 3 independent trials (n = 3 per trial).

The residual buffer with NPs remaining in the dialysis bags at all studied pH levels was analysed by flow cytometry and compared to H-AFt only (control), also placed in a dialysis bag (Figure S4 b). At pH 2 and 4, residual dialysis bag buffer revealed only 2 negative (R4) populations exposing no fluorescence in the histograms relative to control. However at pH 7.5,

a small population positive for fluorescence remained (R3): 18.0 ± 3.1 times brighter fluorescence was detected compared to H-AFt alone, which corroborates to the results obtained by UV spectrometry (Figure S4 c).

Production Data

Click here to download Production Data: Figures 21Aug Final.pptx